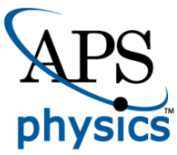

Buckling transition of a semiflexible filament in extensional flow

Harishankar Manikantan and David Saintillan

Phys. Rev. E **92**, 041002 — Published 20 October 2015

DOI: 10.1103/PhysRevE.92.041002

The buckling transition of a semiflexible filament in extensional flow

Harishankar Manikantan and David Saintillan
Department of Mechanical and Aerospace Engineering, University of California San Diego, 9500 Gilman Drive, La Jolla, California 92093-0411, USA

An analytical expression for the fluctuation-rounded stretch-coil transition of semiflexible polymers in extensional flows is derived. The competition between elasticity and tension is known to cause a buckling instability in filaments placed near hyperbolic stagnation points, and the effect of thermal fluctuations on this transition has yet to receive full quantitative treatment. Motivated by the findings of recent experiments as well as our simulations, we solve for the amplitude of the first buckled mode near the onset of the instability. This reveals a stochastic supercritical bifurcation, which is in excellent agreement with full numerical simulations.

The nonlinear dynamics of elastic filaments driven by hydrodynamic forces have received significant attention in recent times, sparked mainly by advances in experiments ranging from the microscopic [1–3] to the macroscopic [4] lengthscales, as well as by the development of efficient low-dimensional models to quantitatively describe them [5–8]. Of particular interest are semiflexible filaments, which are in between the extremities of entropy-dominated floppy polymers and rigid rods in terms of elastic stiffness. Pertinent to the contents of this Rapid Communication is that these particles allow for a competition between bending forces and flow-induced internal stresses, in the presence of thermal fluctuations.

Understanding the configurational transitions of semiflexible filaments is key to deciphering a plethora of dynamics ranging from tumbling [2, 3] to buckling [1, 9] to helical coiling [8], which in turn could result in atypical transport [10, 11] or non-Newtonian behavior [7, 12]. Beside offering rich mechanical properties that enable such dynamics, semiflexible biopolymers are of paramount importance to living cells: eukaryotic cells are structurally supported by a cytoskeletal system comprised of filamentous actin. Configurational transitions in such systems have been suggested to lie at the core of biological pattern formation via self-organizational phenomena such as cytoplasmic streaming [13].

Much like an elastic beam simply loaded at its ends, an elastic filament placed in a viscous fluid can undergo a buckling transition if the hydrodynamic force acting on it overcomes its elastic restoring force. This may be driven by internal forces generated in response to an imposed flow [1, 6–9, 11], or by an external force [14]. Motivated by the recent experiments of Kantsler and Goldstein [1] and by the rising ubiquity of microfluidic trap devices [15] that employ such flows, we focus here on the former scenario — specifically, the buckling transition of a semiflexible filament placed at the stagnation point in a linear hyperbolic flow. Adapting our approach to simple shear is straightforward. Inextensibility of such filaments is ensured by an internal tensile force that acts to resist length changes. It is the competition of this very line tension with bending forces that results in non-trivial shape instabilities, and the effect of thermal fluctuations on such instabilities is the subject of this Rapid Communication.

Euler buckling, wherein an elastic beam is loaded constantly at its ends, is well understood, and recent efforts [16, 17] have shown that the effect of stochastic forces is to smoothen the otherwise sharp transition from a straightened to a buckled configuration. Although we expect a rounded transition in the case of filaments placed in a viscous fluid as well, extending these theories to the fluid-structure interaction problem is not straightforward, primarily due to the *non-uniform* tensile force that drives the buckling instability. In the non-Brownian limit, Young and Shelley [6] were the first to quantify a dynamic instability leading to the so-called *stretch-coil* transition when the driving flow strength exceeds a critical value. Following this, Kantsler and Goldstein [1] comprehensively observed this transition in single actin filaments using microfluidics, and showed that while fluctuations round the bifurcation, it is broadly consistent with the athermal linear predictions. More recently, Deng *et al.* [18] approached the same problem numerically and reported a similar transition. While their simulations captured the effect of Brownian noise on nonlinear filament dynamics, an analytical description of this stochastic bifurcation has yet to receive a quantitative treatment. Here, we present the first mathematical description of the stretch-coil transition in the presence of thermal fluctuations.

We consider a slender, inextensible filament placed in an external flow field of characteristic flow strength $\dot{\gamma}$ in a Stokesian fluid of viscosity μ. The filament has length L and a characteristic radius of cross section $b = \epsilon L$ (with $\epsilon \ll 1$), which defines the slenderness parameter $c = \log(1/\epsilon^2)$. The material of the filament is assumed to be homogeneous with bending rigidity κ, which determines the thermal persistence length $\ell_p = \kappa/k_B T$. This is the lengthscale over which bending forces and thermal forces are comparable, and semiflexible filaments fall in the regime where $\ell_p \sim L$.

The slender-body equation [19] provides a balance between the anisotropic viscous drag on the filament and the internal forces felt along its backbone. Denoting by $\mathbf{x}(s,t)$ the position of the filament centerline at arclength location $s \in [-L/2, L/2]$, and making the system dimensionless using standard methods [11, 20], this balance

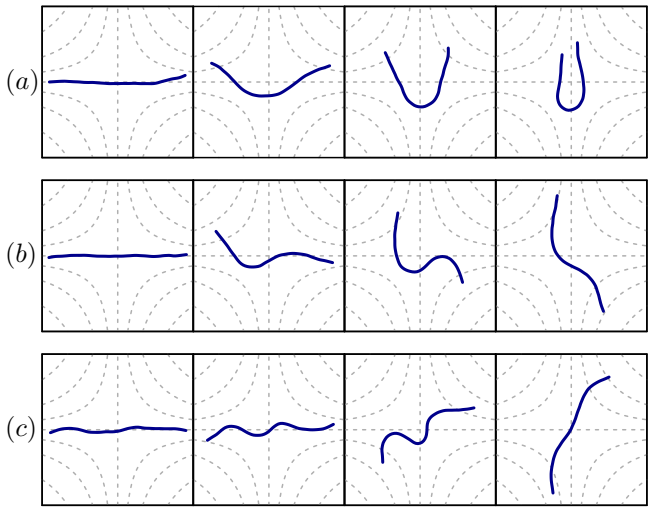

FIG. 1. (Color online) Snapshots from three separate numerical simulations showing typical filament shapes as a result of the buckling instability. Higher modes are observed as we increase the flow strength from (*a*) $\bar{\mu} = 16000$ to (*b*) $\bar{\mu} = 32000$ to (*c*) $\bar{\mu} = 64000$. Streamlines of the hyperbolic flow are shown in dotted lines, and the flow is compressional along the horizontal and extensional along the vertical. The persistence length in each case is $\ell_p = 10\,L$.

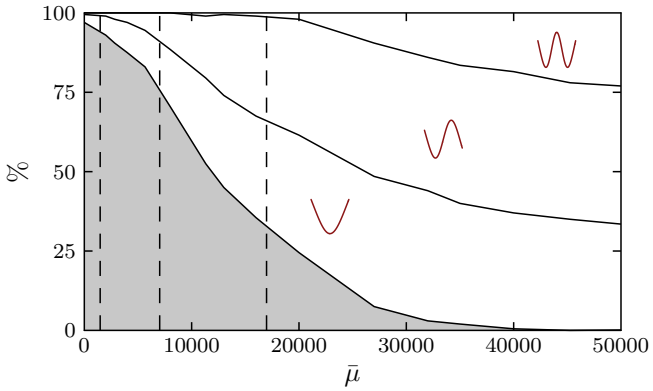

FIG. 2. (Color online) Percentage of excited modes across a range of flow strengths. The vertical dashed lines denote the deterministic thresholds for the first three modes (shapes shown), and the shaded area represents the percentage of cases where no buckling was recorded. All simulations are for $\ell_p/L = 10$. Each vertical section is a distribution across 200 simulations.

reads

$$\mathbf{x}_t(s,t) = \bar{\mu}\mathbf{u}^{\infty}(s,t) - \mathbf{M}(s,t)\cdot\mathbf{f}(s,t). \tag{1}$$

Here, $\mathbf{u}^{\infty}$ is the imposed velocity field, $\bar{\mu} = 8\pi\dot{\gamma}\mu L^4/\kappa$ is a dimensionless flow strength, and subscripts denote partial differentiation with the corresponding variable. $\mathbf{M}(s,t) = \lambda_1\mathbf{I} + \lambda_2\mathbf{x}_s(s,t)\mathbf{x}_s(s,t)$ is a configuration-dependent second-order mobility tensor that captures the local anisotropic drag with $\lambda_1 = c+1$ and $\lambda_2 = c-3$. The force distribution $\mathbf{f}(s,t)$ on the filament has contributions from Euler-Bernoulli elasticity and a fluctuating Brownian term: $\mathbf{f} = -(T\mathbf{x}_s)_s + \mathbf{x}_{ssss} + \mathbf{f}^{br}$. $T(s)$ is the non-uniform line tension, which is not a material property but a Lagrange multiplier acting to ensure filament inextensibility. The Brownian contribution follows from the fluctuation-dissipation theorem and, under the current non-dimensionalization, is such that $\langle\mathbf{f}^{br}(s,t)\rangle = \mathbf{0}$ and $\langle\mathbf{f}^{br}(s,t)\mathbf{f}^{br}(s',t')\rangle = 2(L/\ell_p)\mathbf{M}^{-1}\delta(t-t')\delta(s-s')$.

Simplifying the slender-body equation and using $\mathbf{x}_s\cdot\mathbf{x}_s = 1$ (following inextensibility) and hence $\mathbf{x}_s\cdot\mathbf{x}_{ss} = 0$, one finds

$$\begin{aligned}\mathbf{x}_t = {}& \bar{\mu}\mathbf{u}^{\infty} + \lambda_1 T\mathbf{x}_{ss} + (\lambda_1+\lambda_2)T_s\mathbf{x}_s - \lambda_1\mathbf{x}_{ssss} \\ & - \lambda_2(\mathbf{x}_s\cdot\mathbf{x}_{ssss})\mathbf{x}_s + (\lambda_1\mathbf{I} + \lambda_2\mathbf{x}_s\mathbf{x}_s)\cdot\mathbf{f}^{br}.\end{aligned} \tag{2}$$

The simulations shown in this Rapid Communication follow a Brownian dynamics algorithm [11] that solves Eq. (2). The line tension is unknown *a priori* and is obtained dynamically as a solution to a differential equation that results from applying the identity $(\mathbf{x}_s\cdot\mathbf{x}_s)_t = 0$. Free-end boundary conditions are used to ensure that the total force and torque on the filament be zero: $\mathbf{x}_{ss}|_{s=\pm1/2} = \mathbf{x}_{sss}|_{s=\pm1/2} = T|_{s=\pm1/2} = 0$. For all results reported here, we use an aspect ratio of $\epsilon = 0.01$.

Figure 1 shows snapshots from our simulations, and they resemble the shapes seen in the experiments of Kantsler and Goldstein [1] at corresponding flow strengths (Σ in their notation being equal to $\bar{\mu}/4\lambda_1\pi^4$). When placed along the compressional axis of a sufficiently strong flow, the filament experiences a *negative* tension along its backbone whose balance with viscous, elastic, and thermal forces dictates the observed shapes. As it buckles, it also reorients and eventually aligns with the extensional axis where the now *positive* tension acts to stretch it. Solving for the non-Brownian and linearized dynamics of an initially straight filament in such a flow, Young and Shelley [6] deduced that an instability first occurs at $\bar{\mu}_{cr} \approx 1478$, and that higher modes are destabilized at subsequent thresholds. Experiments as well as our simulations show qualitatively similar modes as the deterministic predictions, albeit with shape fluctuations owing to Brownian kicks. A key difference is that thermal fluctuations excite multiple modes regardless of flow strength by equipartition of energy [1], thus affecting the distribution of modes seen in the event of buckling. To quantify this, we identify the predominant mode whose amplitude grows beyond a noise floor of $0.05\,L$ in 200 different simulations each for various flow strengths. The distribution of excited modes is shown vs $\bar{\mu}$ in Fig. 2, and the trends in dominant shapes, although strongly rounded by fluctuations, are consistent with the deterministic predictions. This is reminiscent of the stochastic Euler buckling problem [16, 17], where thermal fluctuations have been shown to round the transition near the deterministic critical force. This motivates the following analysis where we quantify the transition near the first deterministic threshold, or critical flow strength associ-

ated with the first buckling mode.

To analyze this transition, we first adopt a Monge representation and write $\mathbf{x}(s,t) = (s,h)$ where $h(s,t)$ is the deflection away from the axis of compression in the hyperbolic flow $\mathbf{u}^\infty = (-x, y) = (-s, h)$. Further, we assume that the parabolic form of tension corresponding to a straightened filament placed at the origin holds even when it is deformed — an assumption that is justified for small deflections away from the axis as arise near the onset of buckling. This tension profile can be determined by manipulating Eq. (2) and takes the form $T(s) = \bar{\mu}(s^2 - 1/4)/2(\lambda_1 + \lambda_2)$. Also, since the variable h measures vertical deflections away from the $y = 0$ axis, we consider only thermal fluctuations in this direction. Then, the scalar equation for h reads:

$$\begin{aligned}\frac{\partial h}{\partial t} = \bar{\mu}\left[h + \frac{1}{2}\frac{\lambda_1}{\lambda_1+\lambda_2}\left(s^2 - \frac{1}{4}\right)h_{ss} + sh_s\right] \\ - \lambda_1 h_{ssss} - \lambda_2 h_s^2 h_{ssss} + \sqrt{2\lambda_1\frac{L}{\ell_p}}\,\xi(s,t),\end{aligned} \tag{3}$$

where $\xi(s,t)$ is a white noise with zero mean and correlation $\langle \xi(s,t)\xi(s',t')\rangle = \delta(s-s')\delta(t-t')$.

Ignoring the non-linear and stochastic terms above and assuming a form $h(s,t) = \phi(s)e^{\varsigma t}$ leads directly to the linear stability results of Young and Shelley [6]. Defining the terms within the square brackets in (3) as $\mathcal{L}[h]$, marginal linear stability ($\mathrm{Re}[\varsigma] = 0$) in the non-Brownian case corresponds to the eigenvalue problem

$$\bar{\mu}_{cr}^{(n)}\mathcal{L}[\phi^{(n)}(s)] = \lambda_1\phi_{ssss}^{(n)}(s), \tag{4}$$

where $\phi^{(n)}$ is the n-th buckling mode that is destabilized at a critical flow strength $\bar{\mu}_{cr}^{(n)}$. Since our interest is in the effect of fluctuations near the first buckling transition, we use $n = 1$ from here on and avoid the superscripts. Also, we introduce a parameter m which is the distance from the deterministic threshold: $\bar{\mu} = \bar{\mu}_{cr} + m$. In order to reduce to a form amenable to treatment as a stochastic supercritical bifurcation [21], we introduce the ansatz $h(s,t) = a(t)\phi(s)$ near $\bar{\mu}_{cr}$. Using Eq. (4), the governing equation becomes:

$$\phi\frac{da}{dt} = \frac{m\lambda_1}{\bar{\mu}_{cr}}a\phi_{ssss} - \lambda_2 a^3\phi_s^2\phi_{ssss} + \sqrt{2\lambda_1\frac{L}{\ell_p}}\,\xi. \tag{5}$$

Recall that ϕ and its derivatives solve the eigenvalue problem (4), which admits orthogonal eigenfunctions. Projecting Eq. (5) on the first eigenfunction ϕ then yields a Langevin equation governing the time dynamics of the amplitude $a(t)$:

$$\frac{da}{dt} = m\gamma a - 2\omega a^3 + \sqrt{\sigma}\zeta(t). \tag{6}$$

This is, in fact, a time-dependent stochastic Ginzburg-Landau model for the amplitude of the first buckled mode. Here, $\gamma = \lambda_1 A_1/\bar{\mu}_{cr}$, $\omega = \lambda_2 A_2/2$, and $\sigma = 2\lambda_1 L/\ell_p$ are all positive parameters. A_1 and A_2 are constants that depend on the shape of the eigenfunctions, given respectively by $\int_{-1/2}^{1/2}\phi\phi_{ssss}\,ds$ and $\int_{-1/2}^{1/2}\phi\phi_s^2\phi_{ssss}\,ds$. $\zeta(t) = \int_{-1/2}^{1/2}\xi(s,t)\phi(s)\,ds$ is a normal variate with zero mean and correlation $\langle\zeta(t)\zeta(t')\rangle = \delta(t-t')$.

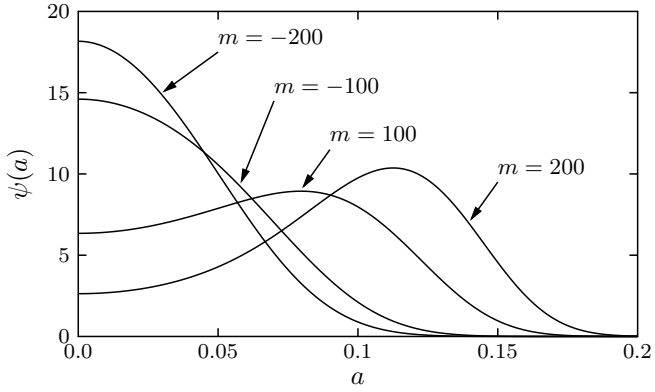

FIG. 3. Probability density of the amplitude a according to Eq. (8) corresponding to $\sigma = 2.04$ ($\ell_p/L = 10$). The deterministic buckling threshold is $m = 0$, and the distribution consistently shift towards higher amplitudes as m increases.

Equation (6) has as its deterministic ($\sigma = 0$) and linear ($\omega = 0$) limit the solution $a(t) \sim \exp[m\gamma t]$, which, consistent with the predictions of the linear stability analysis, decays when $m < 0$ ($\bar{\mu} < \bar{\mu}_{cr}$) and grows otherwise. Analyzing the deterministic yet non-linear problem ($\sigma = 0 \neq \omega$) reveals a supercritical pitchfork bifurcation at $m = 0$ with $a = \sqrt{\gamma m/2\omega}$ when $m > 0$. The stochastic bifurcation will be shown to correctly limit to this form as $\sigma \to 0$.

We now look to quantify the thermal rounding of this bifurcation for finite ℓ_p ($\sigma \neq 0$). We first obtain the Fokker-Planck equation corresponding to Eq. (6), which provides a deterministic equation for the probability density $\psi(a,t)$ of the amplitude a:

$$\frac{\partial\psi}{\partial t} = -\frac{\partial}{\partial a}\left[(m\gamma a - 2\omega a^3)\psi\right] + \frac{\sigma}{2}\frac{\partial^2\psi}{\partial a^2}. \tag{7}$$

A steady solution for the stationary probability density $\psi_S = \psi(t\to\infty)$ can be obtained as

$$\psi_S(a; m, \gamma, \omega, \sigma) = \frac{1}{N}\exp\left[\frac{1}{\sigma}(m\gamma a^2 - \omega a^4)\right], \tag{8}$$

where $N(m,\gamma,\omega,\sigma)$ is a normalization constant such that $\int_0^\infty \psi_S\,da = 1$. The effect of the sign of m is obvious in Eq. (8), shown also in Fig. 3: $\psi_S(a; m \leq 0)$ always peaks at $a = 0$, whereas a positive value of m shifts the peak to a finite positive value of a. The non-linearity is critical as well, as $\omega = 0$ is a Gaussian that always peaks at $a = 0$.

We can now solve for the expected value $\langle a\rangle$ =

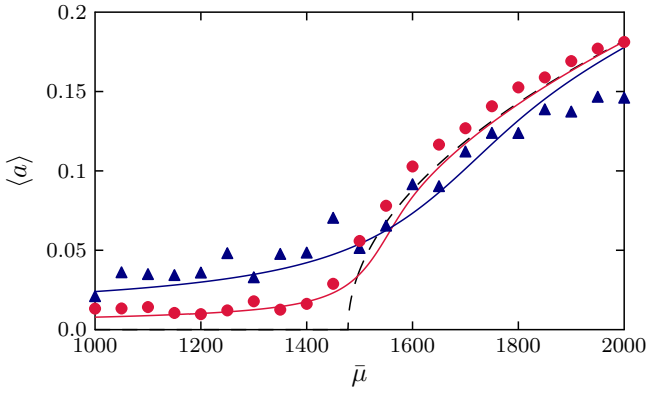

FIG. 4. (Color online) Expected value of the amplitude of the first buckled mode as a function of flow strength. The dashed line is the deterministic pitchfork bifurcation; the solid lines (red for $\ell_p/L = 100$ and blue for $\ell_p/L = 10$) follow Eq. (9) and depart from the sharp transition for increasingly noisy systems. The symbols (red circles for $\ell_p/L = 100$ and blue triangles for $\ell_p/L = 10$) are extracted from simulations without any fitting parameters.

$\int_0^\infty a\psi_S \, da$ of the amplitude, which reads:

$$\langle a \rangle = \frac{1}{\mathcal{G}} \sqrt{\frac{2\sigma}{\gamma|m|\pi}} \exp\left[\frac{\gamma^2 m^2}{8\omega\sigma}\right] \left[1 + \mathrm{erf}\left(\frac{\gamma m}{2\sqrt{\omega\sigma}}\right)\right], \quad (9)$$

where

$$\mathcal{G} = \begin{cases} \dfrac{\sqrt{2}}{\pi} K_{1/4}\left[\dfrac{\gamma^2 m^2}{8\omega\sigma}\right] & : m < 0, \\ I_{-1/4}\left[\dfrac{\gamma^2 m^2}{8\omega\sigma}\right] + I_{1/4}\left[\dfrac{\gamma^2 m^2}{8\omega\sigma}\right] & : m \geq 0, \end{cases} \quad (10)$$

and $I_\nu(x)$ and $K_\nu(x)$ are, respectively, the modified Bessel functions of the first and second kind.

Figure 4 shows the predicted amplitude as the flow strength is varied across the deterministic threshold. Akin to constantly loaded fibers, the effect of thermal fluctuations is to round the sharp transition. Non-trivial modes are excited at arbitrary flow strengths as a consequence of equipartition of energy, and this manifests as a finite amplitude of the first buckled mode well below $\bar{\mu}_{cr}$. Evaluating the limit of (9) as $m \to 0$ indicates that the corresponding expected value is indeed non-zero and varies as $\sigma^{1/4} \sim \ell_p^{-1/4}$, i.e., the amplitude at the deterministic threshold is larger for more flexible filaments. Beyond $\bar{\mu}_{cr}$, $\langle a \rangle$ crosses over and approaches the deterministic pitchfork bifurcation value of $\sqrt{\gamma m/2\omega}$. This approach is slower as ℓ_p decreases, suggesting a larger mean projected length in the buckled state. Recall from Eq. (6) that the finite buckled amplitude in the deterministic case is set by the component of the elastic force along the local tangent vector. The effect of thermal fluctuations beyond the transition is to reduce this amplitude, which can be viewed as an effectively stiffer spring against hydrodynamic compression. This coupling between elasticity and Brownian motion is crucial — an increase in temperature hardens the filament and acts to straighten it out, which is contrary to floppy polymers that are driven solely by configurational entropy and shrink in response to increasing temperature. This again is reminiscent of constantly loaded beams under the influence of thermal fluctuations, where an apparent stretching has been reported past the critical force [16].

In order to test this prediction, we compare it against full numerical simulations of Eq. (2) using a Brownian dynamics algorithm [11]. We place a filament in a hyperbolic flow which is dynamically adjusted to remain compressional along the direction of the end-to-end vector. This eliminates filament reorientation and provides long-time statistics, which are necessary for comparison with the stationary probability distribution derived above. After an initial transience, a stochastically steady state is reached. This is ensemble-averaged and compared to $\phi(s)$ to obtain a numerical prediction for the expected value of a. Higher modes may be excited by thermal fluctuations, and we eliminate these in our averages. The result is shown in Fig. 4 for two different values of ℓ_p and matches excellently with our predictions without any fitting parameters. The simulations also display the smoothed trend in the transition, as well as the apparent pre-buckling softening and post-buckling hardening due to the particular nature of the stochastic bifurcation.

We have analytically quantified the buckling transition of a semiflexible filament in extensional flow as a stochastic supercritical bifurcation, with the resulting expression specifying the exact nature of the finite-temperature rounding of the transition. While this analysis solves a vital facet of fluid-filament interaction problems at the microscale, it also provides a powerful tool for experimentalists to extract mechanical properties of single macromolecules by fitting shape deformations around critical points. The theory presented here, while elaborated for extensional flows, is also sufficiently general to be extended to other flows commonly encountered in microfluidics. For instance, predicting the transition to the first deformed mode in simple shear, often called 'hairpins' [2, 12], is straightforward once the appropriate form of the tension is known [22]. Generalization of the analysis to include multiple modes is an open problem that warrants attention, as is the coupled description of deformation and rotation after buckling.

We thank Raymond E. Goldstein for useful conversations on this work. This work was supported by NSF CAREER grant CBET-1532652.

[1] V. Kantsler and R. E. Goldstein, Phys. Rev. Lett. **108**, 038103 (2012).

[2] M. Harasim, B. Wunderlich, O. Peleg, M. Kröger, and A. R. Bausch, Phys. Rev. Lett. **110**, 108302 (2013).

[3] D. Steinhauser, S. Köster, and T. Pfohl, ACS Macro Lett. **1**, 541 (2012).

[4] E. Wandersman, N. Quennouz, M. Fermigier, A. Lindner, and O. du Roure, Soft Matter **6**, 5715 (2010).

[5] T. R. Powers, Rev. Mod. Phys. **82**, 1607 (2010).

[6] Y.-N. Young and M. J. Shelley, Phys. Rev. Lett. **99**, 058303 (2007).

[7] A.-K. Tornberg and M. J. Shelley, J. Comput. Phys. **196**, 8 (2004).

[8] R. Chelakkot, R. G. Winkler, and G. Gompper, Phys. Rev. Lett. **109**, 178101 (2012).

[9] L. Guglielmini, A. Kushwaha, E. S. G. Shaqfeh, and H. A. Stone, Phys. Fluids **24**, 123601 (2012).

[10] L. Bourdieu, T. Duke, M. B. Elowitz, D. A. Winkelmann, S. Leibler, and A. Libchaber, Phys. Rev. Lett. **75**, 176 (1995); L. Bourdieu, M. O. Magnasco, D. A. Winkelmann, and A. Libchaber, Phys. Rev. E **52**, 6573 (1995).

[11] H. Manikantan and D. Saintillan, Phys. Fluids **25**, 073603 (2013).

[12] I. Kirchenbuechler, D. Guu, N. A. Kurniawan, G. H. Koenderink, and M. P. Lettinga, Nat. Commun. **5**, 5060 (2014).

[13] F. G. Woodhouse and R. E. Goldstein, Proc. Natl. Acad. Sci. U.S.A. **110**, 14132 (2013).

[14] A. A. Evans, S. E. Spagnolie, D. Bartolo, and E. Lauga, Soft Matter **9**, 1711 (2013); L. Li, H. Manikantan, D. Saintillan, and S. E. Spagnolie, J. Fluid Mech. **735**, 705 (2013).

[15] J. Deschamps, V. Kantsler, E. Segre, and V. Steinberg, Proc. Natl. Acad. Sci. U.S.A. **106**, 11444 (2009); M. Tanyeri, M. Ranka, N. Sittipolkul, and C. M. Schroeder, Lab Chip **11**, 1786 (2011).

[16] K. Baczynski, R. Lipowsky, and J. Kierfeld, Phys. Rev. E **76**, 061914 (2007).

[17] M. Emanuel, H. Mohrbach, M. Sayar, H. Schiessel, and I. M. Kulić, Phys. Rev. E **76**, 061907 (2007).

[18] M. Deng, L. Grinberg, B. Caswell, and G. E. Karniadakis, Soft Matter **11**, 4962 (2015).

[19] G. K. Batchelor, J. Fluid Mech. **44**, 419 (1970).

[20] T. Munk, O. Hallatschek, C. H. Wiggins, and E. Frey, Phys. Rev. E **74**, 041911 (2006).

[21] G. Agez, M. G. Clerc, and E. Louvergneaux, Phy. Rev. E **77**, 026218 (2008).

[22] L. E. Becker and M. J. Shelley, Phys. Rev. Lett. **87**, 198301 (2001).